

[Skip to main content](#)

Advertisement



No matter what you're researching, we have an expert for your paper.

Get published faster with high quality English Editing by US PhDs



 Springer

[Search](#) 

- [Authors & Editors](#)
- [My account](#)

Menu

- [Authors & Editors](#)
- [My account](#)
- [Journal home](#) >
- Editors



[Iranian Journal of Science and Technology, Transactions A: Science](#)



Editors

Editor-in-Chief

Gholam Hossein Esslamzadeh
Department of Mathematics
Shiraz University, Iran
e-mail: esslamz@shirazu.ac.ir

Editorial Board

Pere Ara
Department of Mathematics, University of Barcelona, Spain
email: para@mat.uab.es

Sina Asadi
Shiraz University, Iran
email: sinaasadi@shirazu.ac.ir

Mohammad Asadzadeh
Department of Mathematics, Chalmers University of Technology, Sweden
email: mohammad@chalmers.se

Aydin Berenjian
University of Waikato, New Zealand
email: aydinb@waikato.ac.nz

Hamid Reza Esmaeili

Department of Biology, Shiraz University, Iran
email: hresmaeili@shirazu.ac.ir

Gholam Hossein Esslamzadeh
Department of Mathematics, Shiraz University, Iran
email: esslamz@shirazu.ac.ir

Behzad Haghighi
Department of Chemistry, Shiraz University, Iran
email: bhaghighi@shirazu.ac.ir

Mahmoud Hesaaraki
Department of Mathematics, Sharif University of Technology, Iran
email: hesaraki@sharif.edu

Subuhi Khan
Aligarh Muslim University, India
email: subuhi2006@gmail.com

Bahram Khani Robati
Department of Mathematics, Shiraz University, Iran
email: khanirobati@gmail.com

Bahman Kholdebarin
Department of Biology, Shiraz University, Iran
email: bkholdeb@biology.susc.ac.ir

Dariush Kiani
Department of Mathematics, Amirkabir University of Technology, Iran
email: dkiani@aut.ac.ir

Anthony To-Ming Lau
Department of Mathematical and Statistical Sciences, University of Alberta, Canada email: anthonyt@ualberta.ca

Seyed Masoud Nabavizadeh
Department of Chemistry, Shiraz University, Iran
email: nabavi@chem.susc.ac.ir

Ahmad Parsian
Department of Statistics, University of Tehran, Iran
email: ahmad_p@khayam.ut.ac.ir

Ezat Raeisi
Department of Geology, Shiraz University, Iran
email: e_raeisi@yahoo.com

Freydoun Rezakhanlou
Department of Mathematics, University of California, Berkeley, USA
email: rezakhan@math.berkeley.edu

Nozar Samani
Department of Geology; Shiraz University, Iran
email: samani@susc.ac.ir

Ahmad Sheykhi
Department of Physics, Shiraz University, Iran
email: asheykhi@shirazu.ac.ir

Ali Reza Soheili
Department of Mathematics, Ferdowsi University of Mashad, Iran
email: soheili@um.ac.ir

Jafar Vatanparast
Department of Biology, Shiraz University, Iran
email: vatanparast@shirazu.ac.ir

Reza Yousefi
Department of Biology, Shiraz University, Iran
email: ryousefi@shirazu.ac.ir

Abdolnaser Zakery
Department of Physics, Shiraz University, Iran
email: zakeri@physics.susc.ac.ir

[Skip to main content](#)












Iranian Journal of Science and Technology, Transactions A: Science
All Volumes & Issues
ISSN: 1028-6276 (Print) 2364-1819 (Online)

In this issue (36 articles)

Support

1. Research Paper
Screening of Medicinal Plants for Potential Source of L-Asparaginase and Optimization of Conditions for Maximum Extraction and Assay of L-Asparaginase from *Asparagus racemosus*
K. Beulah, K. P. J. Hemalatha Pages 1-6
2. Research Paper
Effects of High Light and Chilling Stress on Photosystem II Efficiency of *Aloe vera* L. Plants Probing by Chlorophyll a Fluorescence Measurements
Ghader Habibi Pages 7-13
3. Research Paper
Fermentation Enhances Redox Protective Activities of *Gymnosporia royleana* Wall. ex Lawson Extracts
Saboon, Muhammad Arshad... Pages 15-23
4. Research Paper
Molecular Identification of Ectomycorrhizal Fungal Communities Associated with Oriental Beech Trees (*Fagus orientalis Lipsky*) in Hyrcanian Forest of Iran
Hamed Aghajani, Seyed Mohammad Hojjati... Pages 25-32
5. Research Paper
Application of Fruit Wastes as Cost-Effective Carbon Sources for Biological Sulphate Reduction
Ali Hussain, Muhammad Amwar Iqbal... Pages 33-41
6. Research Paper
Notes on Water Striders (Heteroptera: Gerridae) in Southwest Iran with a Description of a New Macropterous Form of *Metrocoris communis* (Distant, 1910)
Zohreh Khazaei, Saber Sadeghi Pages 43-48
7. Research Paper
Phytochemical Analysis, Antioxidant, Anticancer and Antibacterial Properties of the Caspian Sea Red Macroalgae, *Laurencia caspica*
Azam Moshfeqh, Ali Salehzadeh... Pages 49-56
8. Research Paper
Molecular Aspects of the Interaction of Organic Solvents and Proteinase K: Kinetics and Docking Studies
E. Yadollahi, B. Shareghi, R. Eslami farsani Pages 57-62
9. Research Paper
Ethnobotanical Knowledge and Population Density of Threatened Medicinal Plants of Nanda Devi Biosphere Reserve, Western Himalaya, India
Vikram S. Negi, R. K. Maikhuri, Ajay Maletha... Pages 63-73
10. Research Paper
Cationic Ring Opening Polymerization of Octamethylcyclotetrasiloxane Using a Cost-Effective Solid Acid Catalyst (Maghnite-H⁺)
Djamel Eddine Kherroub, Mohammed Belbachir... Pages 75-83

11.  Research Paper
Graphene Oxide Nano-Sheets-Supported Co(II)-d-Penicillamine as a Green and Highly Selective Catalyst for Epoxidation of Styrene
Sajjad Keshipour, Mehran Kulaei... Pages 85-94
12.  Research Paper
Kinetics and Optimization Studies of Photocatalytic Degradation of Methylene Blue over Cr-Doped TiO₂ using Response Surface Methodology
P. W. Koh, L. Yulianti, S. L. Lee Pages 95-103
13.  Research Paper
Nanosize Metal Schiff Base Complexes as Precursors for the Preparation of HgO, Co₃O₄ and Mn₃O₄ Nanoparticles
Aliakbar Dehno Khalaji, Shaghayegh Izadi... Pages 105-109
14.  Research Paper
Design and Efficient Synthesis of Novel Biological Benzylidenemalononitrile Derivatives Containing Ethylene Ether Spacers
Enayatollah Sheikhsosseini... Pages 111-117
15.  Research Paper
Equilibrium Dynamics of m-Xylene Removal from Aqueous Solution by Organoclay
Michelle Abonele Apemiye, Chidi Obi... Pages 119-125
16.  Research Paper
Applying a Structural Multivariate Method Using the Combination of Statistical Methods for the Delineation of Geochemical Anomalies
Seyyed Saeed Ghannadpour... Pages 127-140
17. Research Paper
Correcting the Sea Surface Temperature by Data Assimilation Over the Persian Gulf
Mahmud Reza Abbasi, Vahid Chegini... Pages 141-149
18.  Research Paper
Synthetic Catalogue Simulation in Low-Seismicity Regions and Few Instrumental Records in Central Iran Based on Monte Carlo Method
Farzad Moradpouri, Nader Fathianpour... Pages 151-160
19.  Research Paper
The Semi-convergence of GSOR-like Methods for Singular Saddle Point Problems
Huidi Wang Pages 161-171
20.  Research Paper
Periodic and Degenerate Orbits Around the Equilibrium Points in the Relativistic Restricted Three-Body Problem
F. A. Abd El-Salam Pages 173-192



RESEARCH PAPER

Kinetics and Optimization Studies of Photocatalytic Degradation of Methylene Blue over Cr-Doped TiO₂ using Response Surface Methodology

P. W. Koh¹ · L. Yuliaty^{2,3} · S. L. Lee^{1,2}Received: 25 February 2017 / Accepted: 25 November 2017 / Published online: 12 December 2017
© Shiraz University 2017

Abstract

Wastewater containing dyes are difficult to treat attributed to their recalcitrant properties and resistance to biodegradation in conventional activated sludge treatment. Removal of dye via photocatalytic approach appears to be promising. This study was performed to examine the effect of various operating parameters on photocatalytic degradation of methylene blue (MB) over chromium oxide-doped TiO₂ followed by optimization study using response surface methodology (RSM) based on Box–Behnken design (BBD). The experiments were carried out at room temperature under visible light irradiation. The dye photocatalytic degradation followed first-order kinetics with rate constant of 0.0301 h⁻¹. The effects of dopant concentration, sample loading and irradiation time were investigated and their binary interactions were modeled. The high regression R² value of 0.9904 confirmed that the proposed equation fits the experimental data accurately. ANOVA analysis results demonstrated that irradiation time was the most significant individual parameter. Verification test enunciated RSM based on BBD which was suitable to optimize photodegradation of methylene blue over chromium oxide-doped TiO₂ photocatalyst.

Keywords Photodegradation · Titania · Optimization · RSM · BBD

1 Introduction

Dyes are widely used in many industries such as textile, leather tanning, paper production, and food industry. It was reported that the amount of current world dyestuffs production is about 10 million kg per year and 1–2 million kg of active dyes enter the biosphere, either dissolved or suspended in water. Pollution caused by dye-containing wastewater in the environment is of great concern associated to their toxicity, mutagenicity and carcinogenicity

characteristics towards the organisms and microorganisms (Allen et al. 2003).

Traditional dye removal methods such as adsorption, flocculation and nanofiltration are proven to be insufficient and generate secondary pollution (Robinson et al. 2001). On the other hand, the new emerging process like biodegradation through microbial processes approach is not effective towards some azo dyes containing sulfonated aromatic amines (Tan et al. 2005). Removal of dye via photodegradation under visible light seems to be an alternative method due to the fact that most of the dyes have strong adsorption in the visible light region. On top of that, photodegradation is a green chemistry process which is able to utilize free solar light as the activation source and fully mineralization of dyes by changing the toxic dyes to non-toxic inorganic salt, carbon dioxide and water can be achieved (Houas et al. 2001). These reasons attract intensive studies on removing of dyes via photodegradation approach. From the experience, TiO₂ is not only function as a promising bifunctional catalyst (Lee and Hamdan 2008) but it is also considered a good photocatalyst due to

✉ S. L. Lee
slee@ibnusina.utm.my

¹ Department of Chemistry, Faculty of Science, Universiti Teknologi Malaysia (UTM), 81310 Johor Bahru, Johor, Malaysia

² Center for Sustainable Nanomaterials, Ibnu Sina Institute for Scientific and Industrial Research, Universiti Teknologi Malaysia (UTM), 81310 Johor Bahru, Johor, Malaysia

³ Ma Chung Research Center for Photosynthetic Pigments, Universitas Ma Chung, Malang 65151, Indonesia

its high resistance to chemical and photochemical corrosion in aggressive aqueous environment (Koh et al. 2017). To overcome the shortcoming of TiO_2 such as big band gap energy (3.2 eV for anatase) and enhance its photocatalytic activity, TiO_2 can be further modified with transition metal (Han et al. 2009).

Many parameters such as amount of dopant, sample dosage, light irradiation time, pH, light intensity, type of light were reported to affect dye photodegradation over TiO_2 photocatalyst (Akpan and Hameed 2009). However, many studies focused on the effect of certain parameter on the photocatalytic efficiency based on the one-factor-at-one-time approach, meaning that one parameter was varied while the other parameters were made constant. The results could be misleading if there is an interaction existed between the parameters. In addition, the one-factor-at-a-time approach is time consuming and costly since more experiments need to be conducted and more consumption of chemicals is required.

Response surface methodology (RSM) is a statistical design tool which can be used to overcome the aforementioned problems. RSM can be used to develop models from experimental data and can be used to obtain an optimal response (in term of photocatalytic efficiency). It also provides process optimization, prediction of the interaction between several parameters, evaluation of effects of several parameters as well as the optimum conditions searching to attain optimal response. RSM based on central composite design or Box–Behnken design (BBD) has been used to optimize photocatalytic degradation of dyes over different photocatalysts. The previous results showed that the predicted values were closed to the experimental values (Abdullah et al. 2012; Cho and Zoh 2007; Debnath et al. 2015; Vaez et al. 2012).

In the current study, the photocatalytic degradation of methylene blue over chromium oxide-doped TiO_2 under visible light irradiation was evaluated and optimized using RSM involving BBD for the first time. BBD actually is one of the RSM designs and is widely used to optimize the photodegradation of a pollutant. Compared to other commonly used techniques such as Doehlert Matrix and Central Composite Designs, BBD offers a few advantages including that it requires less experimental data point and it has high efficiency when the factor is less than or equal to 3 (Box and Behnken 1960; Ferreira et al. 2007). In addition, BBD does not request designs in which all the parameters are performed at the highest or lowest levels at the same time. Therefore, this design is useful in avoiding experiments conducted in extreme conditions, which might lead to unacceptable results (Ferreira et al. 2007).

As aforementioned, the study of interactions between the parameters of photodegradation of dyes is important. Besides, to the best of our knowledge, there is no report on

optimization of photodegradation of MB over metal oxide modified TiO_2 photocatalyst using RSM based on BBD. The important reaction parameters of dopant concentration, irradiation time and photocatalyst loading were used as the variables for the first time. MB, a cationic dye, was selected as the target pollutant because it is known for its difficulty to be degraded under visible light. In fact, it is often selected as a model dye contaminant to evaluate the photocatalytic activity of photocatalysts (Chen et al. 2010). Chromium oxide was chosen as the dopant to modify TiO_2 because it was reported that Cr– TiO_2 has good activity in photodegrading methylene blue (Koh et al. 2015).

2 Experimental

2.1 Synthesis of Photocatalysts

Chromium oxide-doped TiO_2 was synthesized according to the reported paper (Koh et al. 2014). In the typical synthesis, chromium-doped TiO_2 was prepared as follows: titanium tetraisopropoxide (TTIP) (97%, Aldrich) was mixed with absolute ethanol (99.98%, HMBG) and acetylacetone ($\geq 99\%$, Aldrich) according to the molar ratio 1: 100: 2, respectively. The mixture was stirred for 60 min at room temperature. A required amount of chromium(III) acetylacetonate (97%, Aldrich) in acetylacetone was added to the first mixture and further stirred for 30 min at room temperature followed by evaporation at 353 K. The gel was dried in the oven at 383 K overnight, ground into powder and lastly calcined at 773 K for 5 h. The content of Cr oxide in the photocatalysts was varied from 0.5 to 4 mol%. Samples were denoted as $y\text{Cr-TiO}_2$, where y is referred to mol% of dopant Cr oxide. For comparison purpose, undoped TiO_2 was prepared with same procedure without the addition of Cr precursor.

2.2 Characterizations

The prepared photocatalysts were characterized by X-ray Diffractometer (Bruker Advance D8) with Cu $K\alpha$ radiation ($\lambda = 0.15406$ nm, 40 kV, 40 mA). The samples were scanned in the range from $2\theta = 20^\circ$ – 90° with a scan rate of $0.1^\circ/\text{s}$. Perkin Elmer Ultraviolet–Visible Spectrometer Lambda 900 was used to record diffuse reflectance UV–Visible (DR UV–Vis) spectra with barium sulfate (BaSO_4) as reference.

2.3 Photocatalytic Testing and Kinetic Study

The photocatalytic activity of the prepared photocatalyst was tested via photodegradation of MB under visible light irradiation using halogen fiber optic light illuminator

(Dolan-Jenner MI 157, 150 W). UV longpass filter (400 nm, Edmund Optics) was used to allow only visible light ($\lambda > 400$ nm) irradiated on the dye solution. Sample (0.1 g) was put into the beaker consisting of 50 mL 15 ppm of MB and subjected to light illumination for 24 h at room temperature. Adsorption test was carried out prior to photocatalytic study. After the photocatalytic reaction, the solution was centrifuged and the supernatant was withdrawn. The concentration of MB was determined using UV–Vis spectrometer (ThermoFisher, Genesys 10S) at $\lambda = 665$ nm. The photocatalytic activity was calculated using the following equation:

$$\text{Decolorization percentage} = (C_0 - C) / C_0 \times 100\%, \quad (1)$$

where C_0 and C are the concentration of MB before and after the photocatalytic reaction, respectively. Similar experimental conditions were used to study the effect of photocatalyst loading by varying the amount of photocatalyst from 0.0125 to 0.1250 g. On the other hand, different irradiation times (0–24 h) were applied for studying the effect of irradiation time.

2.4 Optimization Study

Photodegradation of MB was optimized by RSM using BBD with three effective variables including dopant concentration, A , irradiation time, B , and photocatalyst loading, C . The statistical software (Design-Expert Version 7) was utilized for the analysis. The following quadratic Eq. 2 was used for the optimization process. The response variable (percent of photodegradation) was fitted with full quadratic model as shown in Eq. 2 in order to correlate it to the experimental variables.

$$Y = \beta_0 + \sum \beta_i x_i + \sum \beta_{ii} x_i^2 + \sum \beta_{ij} x_i x_j \quad (2)$$

where Y is the response variable (percent of photodegradation), and β_0 , β_i , β_{ii} , β_{ij} are coefficients of the intercept, linear, square and interaction effects, respectively. Meanwhile, x_i and x_j are coded independent variables. The validity of the design model was evaluated using ANOVA analysis. It was performed based on the proposed model to find out the interaction between the selected variables and the response. The F value (Fisher variation ratio) and p value (significant probability value) were used to determine the significance of the model; p value of selected model should be less than 0.05% and lack of fit should be insignificant. Meanwhile, the coefficient of determination (R^2) must be close to 1 to indicate the good correlation between the experiment and the predicted values. Three-dimensional contour plots were drawn to visualize the

interaction between the effects of independent variables towards photodegradation of MB.

3 Results and Discussion

3.1 Structural and Optical Properties

As shown in Fig. 1a (a), the TiO_2 was successfully synthesized with purely anatase and body-centered tetragonal in shape (JCPDS 21-1272). Similarly, pure anatase of TiO_2 was obtained via sol–gel method in a previous report (Wu and Chen 2004). When Cr oxide amount was 1 mol% or higher, new diffraction peaks at $2\theta = 27.5^\circ$ and 42.5°

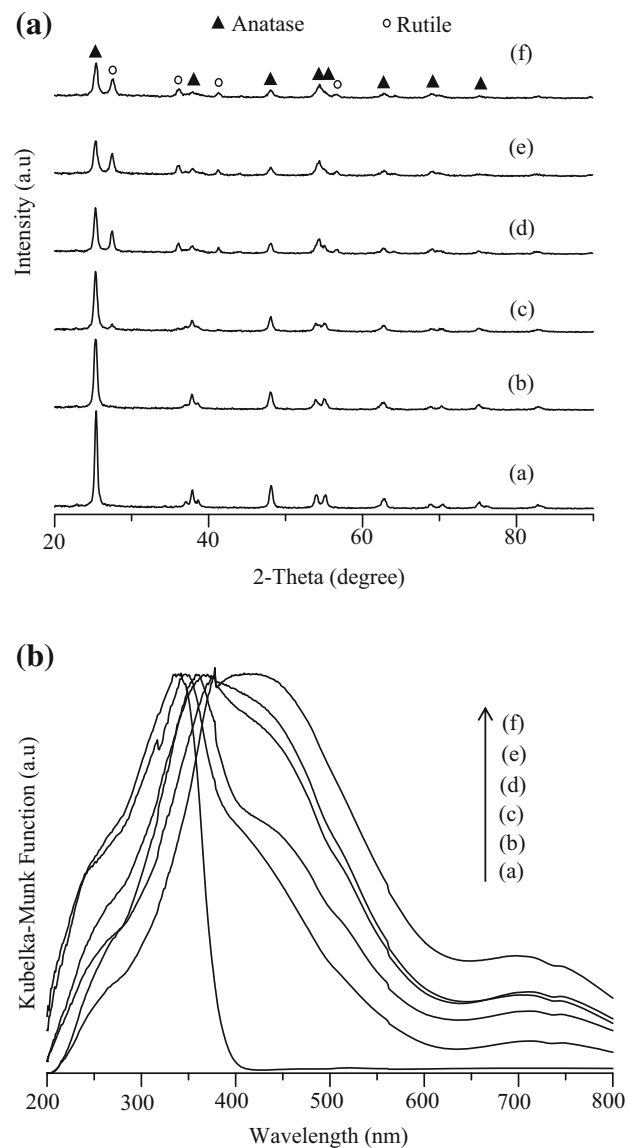


Fig. 1 **a** XRD patterns and **b** DR-UV-Vis spectra of *a* undoped TiO_2 , *b* 0.5Cr- TiO_2 , *c* 1Cr- TiO_2 , *d* 2Cr- TiO_2 , *e* 3Cr- TiO_2 , *f* 4Cr- TiO_2

assigned to rutile peaks (JCPDS 21-1276) were observed, suggesting occurrence of anatase to rutile phase transition. The intensity of these peaks increased as the amount of dopant increased. No Cr oxide peak was detected inferring that the Cr oxide was either too little to be detected or the dopant was highly dispersed on the surface of TiO_2 (Wu and Chen 2004).

As illustrated in Fig. 1b (a), undoped TiO_2 showed typical absorption shoulder at the range of 200–260 nm and absorption peak in the range 320–360 nm which were attributed to tetrahedral and octahedral Ti, respectively (Astorino et al. 1995). Doping of Cr oxide shifted the absorption edge to visible light region suggesting that the synthesized samples could be active under visible light irradiation.

3.2 Photocatalytic Testing

3.2.1 Effect of Dopant Concentration

Photodegradation test using 15 ppm of MB as targeted pollutant was carried out on Cr oxide-doped TiO_2 samples. Adsorption test was carried out over Cr oxide-doped TiO_2 samples prior to the photodegradation to ensure adsorption equilibrium has been achieved. Figure 2 shows the net photodegradation of MB over undoped TiO_2 and Cr oxide-doped TiO_2 at the function of different mole percentage of Cr oxide. After 24 h of light irradiation, it was observed

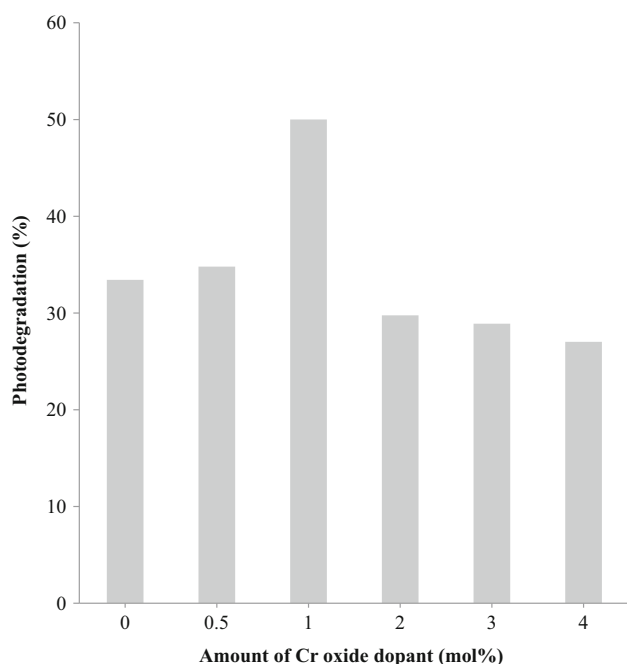


Fig. 2 Photodegradation of MB over Cr oxide-doped TiO_2 of different Cr oxide mol% (Concentration of MB = 15 ppm, irradiation duration = 24 h)

that 33.4% of MB was photodegraded by undoped TiO_2 (pure anatase), even though UV longpass filter (400 nm, Edmund Optics) was used. This could be explained by dye sensitization whereby visible light induced excitation of electron from the highest occupied molecular orbital (HOMO) to the lowest unoccupied molecular orbital (LUMO) of dye molecule and then electron ejected onto conduction band of TiO_2 and ultimately induced photodegradation of MB on TiO_2 surface (Yu et al. 2010).

As shown in Fig. 2, the photodegradation of MB slightly improved after doping with 0.5 mol% Cr oxide. The improvement could be mainly due to dye sensitization effect between MB and TiO_2 and slightly affected by the presence of rutile phase and extended absorption edge to visible light region resulted from addition of Cr oxide (Koh et al. 2017). The optimum amount of Cr oxide dopant was 1 mol% which gave the highest activity of 50%. Further addition of Cr oxide dopant retarded the photocatalytic activity, which could be attributed to the excess of dopant covered the active site of TiO_2 .

3.2.2 Effect of Irradiation Time

Since 1Cr- TiO_2 was the best photocatalyst, the effect of irradiation time on the performance of photodegradation of MB over 1Cr- TiO_2 was studied and the results are depicted in Fig. 3. Upon visible light irradiation, the concentration of MB continued to decrease when the irradiation time was prolonged. Prolonged irradiation time not only enabled more MB dye molecules photosensitized TiO_2 , but also activated Cr- TiO_2 to generate more hydroxyl and

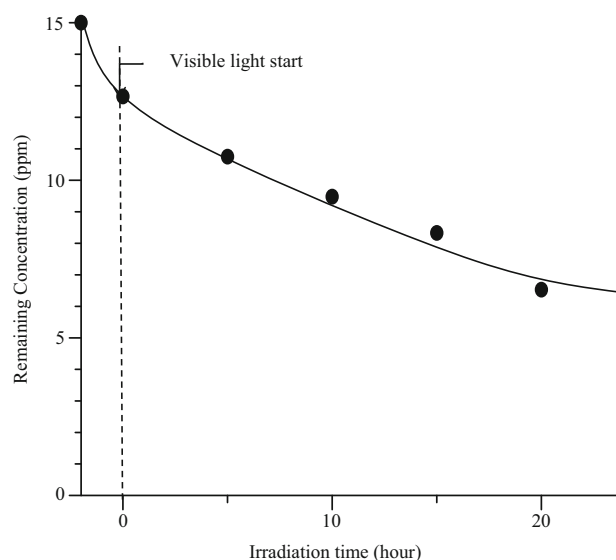


Fig. 3 Effect of irradiation time on the photodegradation of MB (photocatalyst loading = 0.1 g, initial concentration of MB = 15 ppm, photocatalyst used = 1Cr- TiO_2)

superoxide radicals, leading to increase of photodegradation of MB (Akpan and Hameed 2009).

The kinetic order of reaction was investigated. First-order kinetic was plotted according to Eq. 3

$$\ln C_o/C = kt, \tag{3}$$

where C_o is the initial concentration of MB (15 ppm), C is the concentration of MB at time t , k is the rate constant (h^{-1}) and t is the reaction time (hour). As shown in Fig. 4, the data fitted well the first-order kinetic of reaction with the regression coefficient, R^2 equals to 0.985. The obtained rate constant was 0.0301 h^{-1} .

3.2.3 Effect of Photocatalyst Loading

The effect of photocatalyst loading is depicted in Fig. 5. The photodegradation increased from 33.8% to maximum of 50% when the sample loading increased from 0.0125 to 0.1000 g. The enhanced photodegradation when the amount of sample loading increased was probably due to rise in the number of active sites for both photocatalytic and adsorption, hence leading to the improved photocatalytic activity as well as photosensitization effect of 1Cr-TiO₂. However, further increase of sample loading has slightly inversed outcome on the photodegradation of MB. The phenomenon could be attributed to blocking of visible light penetration from reaching the photocatalyst's surface which retarded the photocatalytic activity (Sun et al. 2008).

3.2.4 Response Surface Study

Box–Behnken design was used to study the photodegradation of MB. The effective parameters studied were

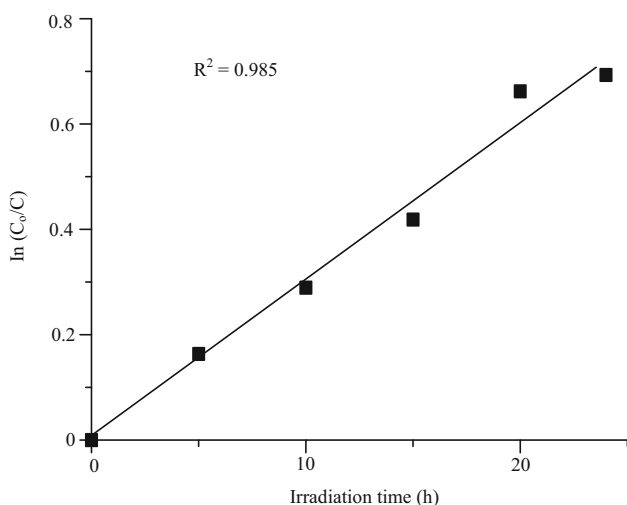


Fig. 4 First-order transforms of photodegradation of MB by 1Cr-TiO₂ photocatalyst under visible light irradiation for 24 h

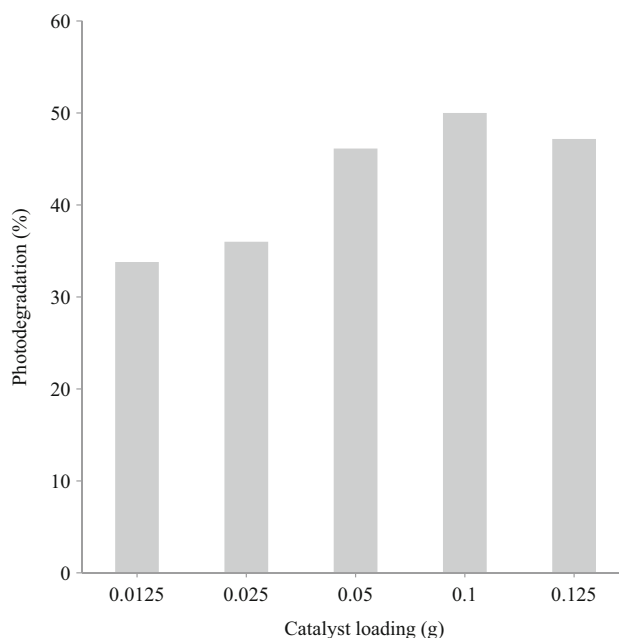


Fig. 5 Effect of photocatalyst (1Cr-TiO₂) loading on the photodegradation of MB (initial MB concentration = 15 ppm, irradiation time = 24 h)

dopant concentration, A (0–2 mol %), irradiation time, B (16–24 h), sample loading, C (0.05–0.14 g). A total of 17 experiments were obtained at random to study the optimize parameters and maximize the photocatalytic degradation of MB. The experimental and predicted values are tabulated

Table 1 Box–Behnken design matrix

Observation	Actual values			Photodegradation of MB (%)		
	A	B	C	Y_{exp}	Y_{pred}	Residual
1	1.00	16.00	0.14	30.88	30.99	- 0.11
2	0.00	24.00	0.10	36.99	37.45	- 0.46
3	1.00	20.00	0.10	50.42	50.70	- 0.28
4	0.00	16.00	0.10	32.08	32.27	- 0.19
5	1.00	20.00	0.10	51.11	50.70	0.41
6	0.00	20.00	0.05	31.15	30.80	0.35
7	0.00	20.00	0.14	32.11	31.80	0.31
8	1.00	24.00	0.05	49.84	49.73	0.11
9	1.00	24.00	0.14	39.91	39.76	0.15
10	1.00	16.00	0.05	37.98	38.13	- 0.15
11	2.00	20.00	0.05	35.16	35.47	- 0.31
12	2.00	24.00	0.10	37.76	37.56	0.20
13	1.00	20.00	0.10	50.93	50.70	0.23
14	2.00	20.00	0.14	17.01	17.36	- 0.35
15	1.00	20.00	0.10	50.02	50.70	- 0.68
16	2.00	16.00	0.10	22.83	22.37	0.46
17	1.00	20.00	0.10	51.02	50.70	0.32

in Table 1. According to the RSM based on BBD, an empirical mutual relationship between the response (photodegradation of MB) and independent parameters is shown in quadratic Eq. 4:

$$Y = 50.70 - 2.45A + 5.09B - 4.28C + 2.50AB - 4.78AC - 0.71BC - 14.54A^2 - 3.75B^2 - 7.30C^2. \quad (4)$$

The plot of predicted versus actual response value is shown in Fig. 6a. The straight line with high regression R^2 value of 0.9904 showed that the predicted value was close to the actual value. The analysis of the residuals which was the difference between obtained experimental and the predicted values was carried out. It gave useful information about the suitability of the model. This analysis identifies the outlier and examined diagnostic plots such as normal probability and residuals plots. The normal probability plot shows whether the residuals follow a normal distribution, in which case the points would follow a straight line (Jawad et al. 2015). From Fig. 6b, the data points could be resembled with a straight line, denoting the residual was normally distributed. On the other hand, the residual versus predicted response value tests the assumption of constant variance. The plot should be in random scatter with a constant range of residuals within the residual range. From Fig. 6c, the pattern of the residuals fluctuated in a random pattern around the centre of the line and within the boundary, meaning that there was no outlier.

The ANOVA analysis is shown in Table 2. The high correlation coefficients ($R^2 = 0.9904$ and adjusted $R^2 = 0.9976$) were obtained which demonstrated close fit between the predicted and experimental values. The high model F value of 749.46 and low p values (less than 0.0500) in the current study indicated the significance of the model. Values of $p > F$ less than 0.0500 suggested that the model terms are significant. Thus, in this case, A , B , C , AB , AC , BC , A^2 , B^2 , and C^2 are significant model terms. From the ANOVA analysis, the lack of fit is not significant. As can be seen in Table 2, the obtained F values for effect of dopant concentration, irradiation time and sample loading are 180.49, 781.79 and 551.85, respectively, showing that the irradiation time was the most significant parameter, followed by sample loading and dopant concentration. By comparing the interactive model term, AC has the highest F value of 344.20, followed by AB (94.63) and BC (7.55), indicating that the interaction of AC was the most significant towards photodegradation of MB.

The response surface plot in three dimensional was plotted to show the interaction between the two parameters towards the photodegradation of MB. In this approach, two parameters were varied within the experimental ranges while another one parameter was kept constant. The 3-D surface plot of photodegradation of MB as a function of dopant concentration and irradiation time is shown in Fig. 7a. The sample loading was kept at 0.1 g. The elliptical shape of the contour plot indicated that the interaction of dopant concentration and irradiation time was effective

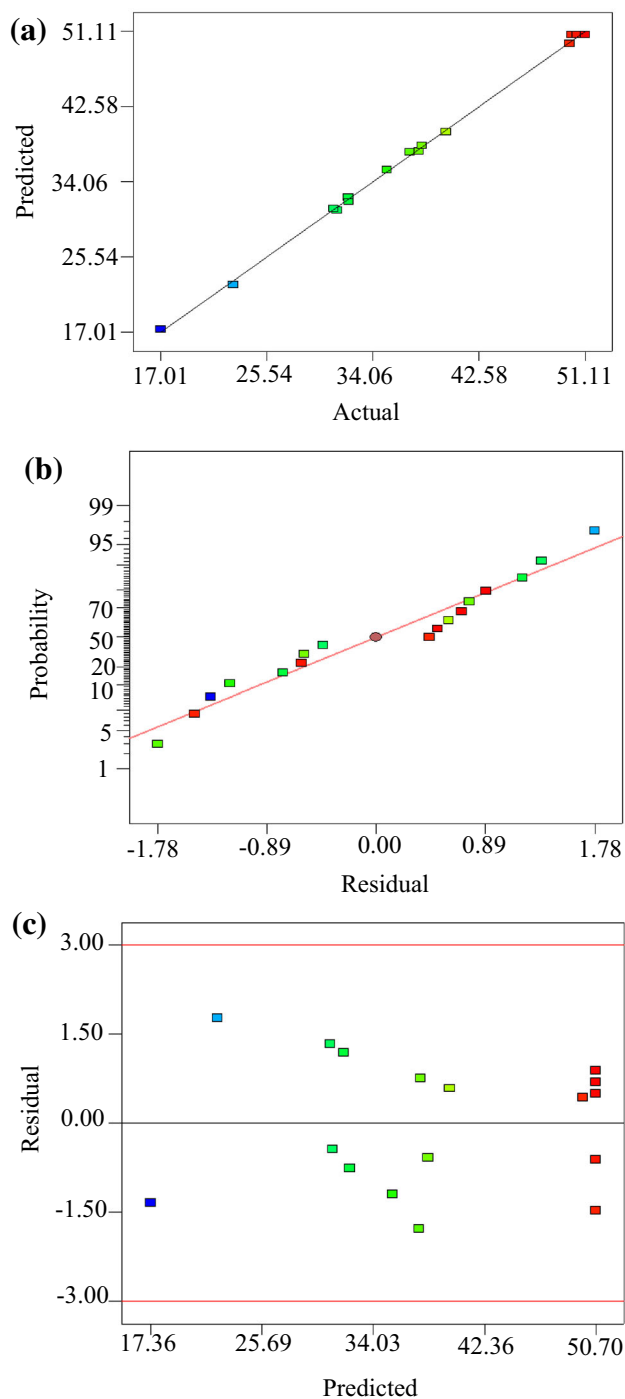


Fig. 6 a Comparison of the predicted and actual value, b Normal probability plot, c Residual versus predicted response values for photodegradation of MB

Table 2 Analysis of variance (ANOVA) for photodegradation of MB

Source	DF	SS	MS	<i>F</i>	<i>p</i>	Remarks
Model ^a	9	1789.12	198.79	749.46	< 0.0001	Significant
Dopant concentration, <i>A</i>	1	47.87	47.87	180.49	< 0.0001	
Irradiation time, <i>B</i>	1	207.37	207.37	781.79	< 0.0001	
Sample loading, <i>C</i>	1	146.38	146.38	551.85	< 0.0001	
<i>AB</i>	1	25.10	25.10	94.63	< 0.0001	
<i>AC</i>	1	91.30	91.30	344.20	< 0.0001	
<i>BC</i>	1	2.00	2.00	7.55	0.0286	
<i>A</i> ²	1	890.15	890.15	3355.95	< 0.0001	
<i>B</i> ²	1	59.05	59.05	222.63	< 0.0001	
<i>C</i> ²	1	224.53	224.53	846.51	< 0.0001	
Residual	7	1.86	0.27			
Lack of fit	3	0.99	0.33	1.53	0.3363	Not significant
Pure error	4	0.86	0.22			
Total	16	1790.98				

DF degree of freedom of different source, *SS* sum of square, *MS* mean of square, *F* degree of freedom, *P* probability

^aPred *R*-squared 0.9904; Adj *R*-squared = 0.9976

towards photodegradation of MB. As shown, when dopant concentration increased, increase of irradiation time enhanced the photodegradation of MB. In the literature, RSM was used to optimize the photocatalytic performance of TiO₂ in degradation of azo pyridine dye under simulated sun light (Dostanić et al. 2013). The authors claimed that irradiation time has the greatest impact towards the photocatalytic activity, followed by oxidant concentration and photocatalyst amount. This could be explained that longer irradiation time devoted to the reaction, the more exposure of Cr–TiO₂ photocatalyst's surface to visible light (Sohrabi and Akhlaghian 2016), and hence produced more hydroxyl radical which photodegraded more MB. On the other hand, even though irradiation time increased, photodegradation of MB increased only with dopant concentration up to 1 mol%. Further increase in dopant concentration reduced the photodegradation of MB. This was because the excess Cr oxide (more than 1 mol%) dopant acted as recombination centre.

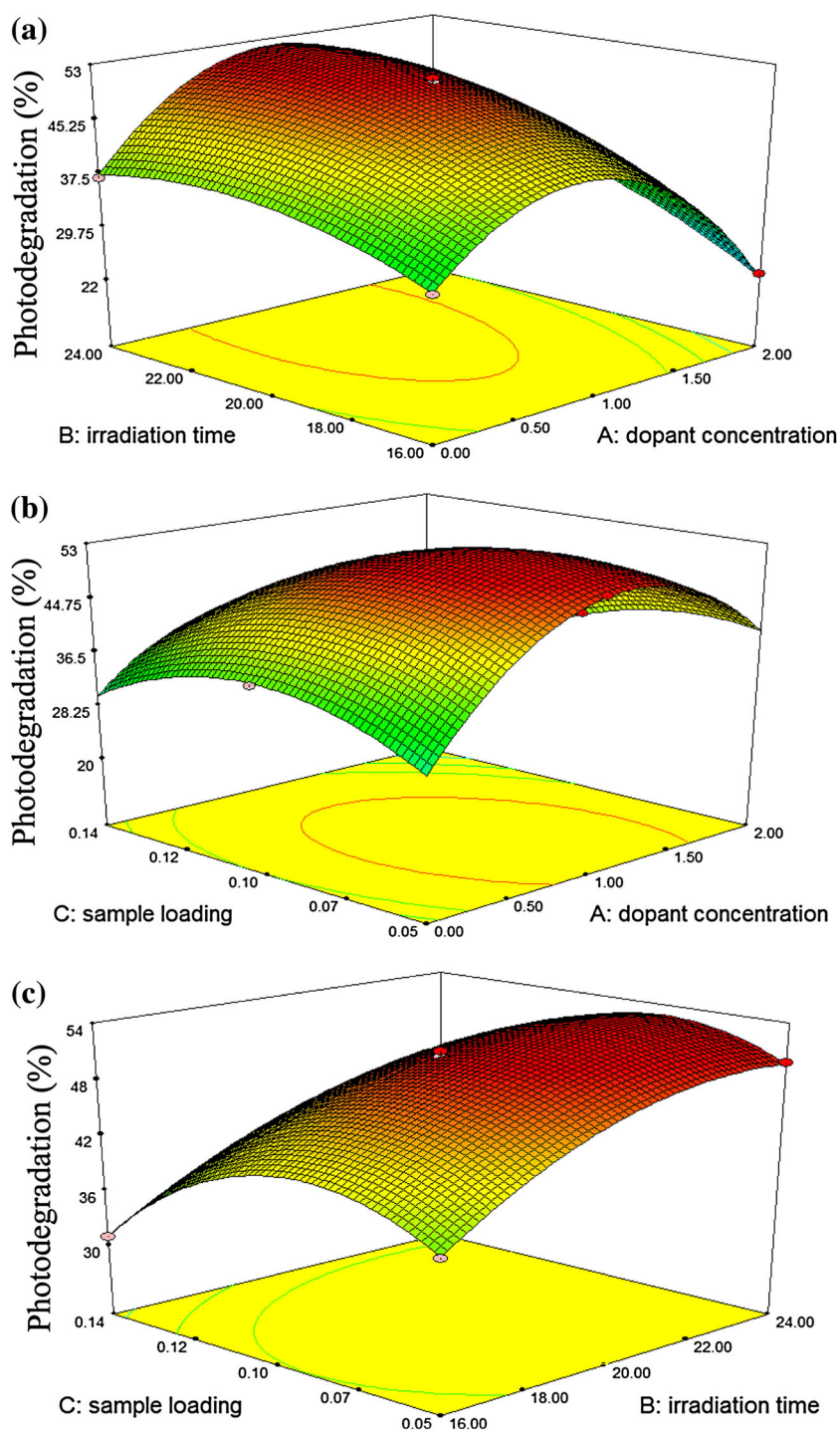
Figure 7b represents the effect of dopant concentration and sample loading towards the photodegradation of MB with keeping the irradiation time at 24 h. It can be seen that increasing dopant concentration up to 1 mol%, and sample loading from 0.05 to 0.1 g improved the photodegradation of MB. On the other hand, further increase in dopant concentration from 1 to 2 mol%, and 0.1 to 0.14 g, retarded the photodegradation of MB. The reason why 1 mol% was the optimum dopant concentration has been given. The photocatalytic degradation of MB increased with increasing sample in the reaction which was mainly due to more active site available to photodegrade MB. Meanwhile, the adverse consequence of excess sample loading would limit

the light reaching the photocatalyst surface leading to decrease of photocatalytic activity. As compared to sample loading, obviously, dopant concentration is more considerable in the photodegradation of MB.

The interaction between irradiation time and sample loading with keeping the dopant concentration at 1 mol% is shown in Fig. 7c. The results showed that at short irradiation time (16 h), increase in sample loading up to approximately 0.1 g increased the photodegradation of MB. Further increase in sample loading retarded the photocatalytic activity. Similar trend was observed even though longer irradiation time was used. Overall, the degree of importance of these three parameters on photodegradation of MB was in descending order of irradiation time > sample loading > dopant concentration.

To obtain the optimized conditions for the photodegradation of MB, the lower and upper limits of each parameter were adjusted to achieve the maximum response. The operational parameters were set to values within the studied range, while the response was set to achieve maximum value. The obtained value of photodegradation of MB was 53.09% at dopant concentration of 0.95 mol%, 23.12 h of irradiation time and 0.08 g of photocatalyst amount, with high desirability of 1. An additional experiment was carried out under the suggested optimum conditions and the obtained photodegradation of MB was 51.78%, which was closely agreed with the predicted result by RSM. The results hence validated the findings of RSM for MB photodegradation over 1Cr–TiO₂.

Fig. 7 3-D surface plots of photodegradation of MB as a function of **a** dopant concentration and irradiation time, **b** dopant concentration and sample loading, **c** irradiation time and sample loading



4 Conclusion

Chromium oxide-doped TiO_2 was efficient photocatalyst for MB photodegradation under visible light irradiation. The reaction followed first-order kinetics with a rate constant of 0.0301 h^{-1} . The results of this study demonstrated that RSM based on BBD could be efficiently used for the modeling and optimization of the photocatalytic

degradation of the dye. Analysis of variance showed a high correlation coefficients ($R^2 = 0.9904$ and adjusted $R^2 = 0.9976$), thus confirming a satisfactory adjustment of the regression model with the experimental data. The current study indicated that the most significant effect on MB photodegradation was found to be irradiation time, followed by photocatalyst loading, while the influence of dopant concentration was the least important. According to

the statistical design method, the optimal photodegradation conditions were determined at 0.95 mol % Cr oxide dopant, 23.12 h of irradiation time, and 0.08 g of photocatalyst loading. Verification experiment was conducted at suggested optimum conditions and the obtained photodegradation value (51.78%) was closely agreed with the predicted value (53.09%). Besides, interaction between dopant concentration and photocatalyst loading was the most significant impact towards photodegradation of MB over Cr-doped TiO₂ under visible light irradiation.

Acknowledgements The authors gratefully acknowledge the Ministry of Higher Education, Malaysia (MOHE) and Universiti Teknologi Malaysia (UTM) for the Research University Grants (vote no.: and Q.J130000.2526.12H77, Q.J130000.2526.13H52 and Q.J130000.21A2.03E61). P. W. Koh is grateful for the MyPhD scholarship from the Ministry of Science, Technology and Innovation, Malaysia (MOSTI).

References

- Abdullah AH, Moey HJM, Yusof NA (2012) Response surface methodology analysis of the photocatalytic removal of methylene blue using bismuth vanadate prepared via polyol route. *J Environ Sci* 24:1694–1701
- Akpan UG, Hameed BH (2009) Parameters affecting the photocatalytic degradation of dyes using TiO₂-based photocatalysts: a review. *J Hazard Mater* 170:520–529
- Allen SJ, Gan Q, Matthews R, Johnson PA (2003) Comparison of optimised isotherm models for basic dye adsorption by kudzu. *Bioresour Technol* 88:143–152
- Astorino E, Peri JB, Willey RJ, Bisca G (1995) Spectroscopic characterization of silicalite-1 and titanium silicate-1. *J Catal* 157:482–500
- Box GEP, Behnken DW (1960) Some new three level designs for the study of quantitative variables. *Technometrics* 2:455–475
- Chen C, Ma W, Zhao J (2010) Semiconductor-mediated photodegradation of pollutants under visible-light irradiation. *Chem Soc Rev* 39:4206–4219
- Cho I-H, Zoh K-D (2007) Photocatalytic degradation of azo dye (reactive red 120) in TiO₂/UV system: optimization and modeling using a response surface methodology (RSM) based on the central composite design. *Dyes Pigm* 75:533–543
- Debnath S, Ballav N, Nyoni H, Maity A, Pillay K (2015) Optimization and mechanism elucidation of the catalytic photo-degradation of the dyes eosin yellow (EY) and naphthol blueblack (NBB) by a polyaniline-coated titanium dioxide nanocomposite. *Appl Catal B: Environ* 163:330–342
- Dostanić J, Lončarević D, Rožić L, Petrović S, Mijin D, Jovanović DM (2013) Photocatalytic degradation of azo pyridone dye: optimization using response surface methodology. *Desalin Water Treat* 51:2802–2812
- Ferreira SLC et al (2007) Box–Behnken design: an alternative for the optimization of analytical methods. *Anal Chim Acta* 597:179–186
- Han F, Kambala VSR, Srinivasan M, Rajarathnam D, Naidu R (2009) Tailored titanium dioxide photocatalysts for the degradation of organic dyes in wastewater treatment: a review. *Appl Catal A* 359:25–40
- Houas A, Lachheb H, Ksibi M, Elalou E, Guillard C, Herrmann JM (2001) Photocatalytic degradation pathway of methylene blue in water. *Appl Catal B: Environ* 31:145–157
- Jawad AH, Alkarkhi AFH, Mubarak NSA (2015) Photocatalytic decolorization of methylene blue by an immobilized TiO₂ film under visible light irradiation: optimization using response surface methodology (RSM). *Desalin Water Treat* 56:161–172
- Koh PW, Yuliati L, Lee SL (2014) Effect of transition metal oxide doping (Cr Co, V) in the photocatalytic activity of TiO₂ for congo red degradation under visible light. *J Teknol* 69:45–50
- Koh PW, Yuliati L, Lintang HO, Lee SL (2015) Increasing rutile phase amount in chromium-doped titania by simple stirring approach for photodegradation of methylene blue under visible light. *Aust J Chem* 68:1129–1135
- Koh PW, Hatta MHM, Ong ST, Yuliati L, Lee SL (2017) Photocatalytic degradation of photosensitizing and non-photosensitizing dyes over chromium doped titania photocatalysts under visible light. *J Photochem Photobiol A: Chem* 332:215–223
- Lee SL, Hamdan H (2008) Sulfated silica-titania aerogel as bifunctional oxidative and acidic catalyst in the synthesis of diols. *J Non-Cryst Solids* 354:3939–3943
- Robinson T, McMullan G, Marchant R, Nigam P (2001) Remediation of dyes in textile effluent: a critical review on current treatment technologies with a proposed alternative. *Bioresour Technol* 77:247–255
- Sohrabi S, Akhlaghian F (2016) Modeling and optimization of phenol degradation over copper-doped titanium dioxide photocatalyst using response surface methodology. *Process Saf Environ Prot* 99:120–128
- Sun J, Qiao L, Sun S, Wang G (2008) Photocatalytic degradation of orange G on nitrogen-doped TiO₂ catalysts under visible light and sunlight irradiation. *J Hazard Mater* 155:312–319
- Tan NCG et al (2005) Fate and biodegradability of sulfonated aromatic amines. *Biodegrad* 16:527–537
- Vaez M, Moghaddam AZ, Alijani S (2012) Optimization and modeling of photocatalytic degradation of azo dye using a response surface methodology (RSM) based on the central composite design with immobilized titania nanoparticles. *Ind Eng Chem Res* 51:4199–4207
- Wu JCS, Chen CH (2004) A visible-light response vanadium-doped titania nanocatalyst by sol-gel method. *J Photochem Photobiol A: Chem* 163:509–515
- Yu L, Yuan S, Shi L, Zhao Y, Fang J (2010) Synthesis of Cu²⁺ doped mesoporous titania and investigation of its photocatalytic ability under visible light. *Micropor Mesopor Mater* 134:108–114